Supporting Information

Probing Spatial Coupling of Resistive Modes in Porous Intercalation Electrodes through Impedance Spectroscopy

Aashutosh N. Mistry and *Partha P. Mukherjee*[*]

School of Mechanical Engineering, Purdue University, West Lafayette, IN 47907, United States

The document presents the mathematical details of the concentrated solution theory which is the cornerstone of electrolyte response in Li-ion battery (LIB) system. Next, the double layer interactions and how all these jointly contribute to electrode impedance response are outlined.

1. Concentrated Solution Theory based Electrolyte Transport Description
2. Electrochemical Response of a Double Layer
3. Mathematical Details of Electrode Impedance
4. Impedance for a Multivalent Intercalation Chemistry

S1. Concentrated Solution Theory Based Electrolyte Transport Description

Typical Li-ion battery electrolyte is prepared by dissolving a lithium salt, e.g., $LiPF_6$ in an organic solvent(s). For the sake of generality, let this salt be $Li_{\nu_p}X_{\nu_n}$ with stoichiometric coefficients ν_p, ν_n and anion X^{z_n}. Appropriate salt dissolution equilibrium is:

$$Li_{\nu_p}X_{\nu_n} \rightleftharpoons \nu_p Li^{z_p} + \nu_n X^{z_n} \tag{S1}$$

The electrolyte consists of three species:

$$\left.\begin{array}{c} p\text{, cation: } Li^{z_p} \\ n\text{, anion: } X^{z_n} \\ s\text{, solvent} \end{array}\right] \tag{S2}$$

Charge neutrality is ensured in an electrolyte everywhere except inside the double layers:

$$\nu_p z_p + \nu_n z_n = 0 \tag{S3}$$

When the electrolyte is prepared, one can only alter salt concentration, C. Ionic concentrations are subsequently defined through their association with stoichiometries:

$$C = \frac{C_p}{\nu_p} = \frac{C_n}{\nu_n} \tag{S4}$$

And the statement of charge neutrality can be mathematically expressed as:

$$C_p z_p + C_n z_n = 0 \tag{S5}$$

[*] Email: pmukherjee@purdue.edu

Let electrochemical potentials of the species (chemical potential for charge-less species) be noted by μ. Gibbs – Duhem relation correlates these thermodynamic quantities with concentrations as follows:

$$C_p \nabla \mu_p + C_n \nabla \mu_n + C_s \nabla \mu_s = 0 \tag{S6}$$

The salt dissolution equilibrium (S1) correlates salt's chemical potential with individual ionic electrochemical potentials via stoichiometries:

$$\mu = \nu_p \mu_p + \nu_n \mu_n \tag{S7}$$

This gives an alternative expression of the Gibbs – Duhem relation:

$$C \nabla \mu + C_s \nabla \mu_s = 0 \tag{S8}$$

Electrochemical potentials of each of the ionic species are related to their respective concentrations, individual activities, and local electric potential[1]. The gradient in salt's chemical potential exhibits the following dependence:

$$\begin{aligned} \nabla \mu &= \nu_p \nabla \mu_p + \nu_n \nabla \mu_n \\ &= \nu RT \nabla \left(\ln \left(f C \right) \right) \\ \nabla \mu &= \nu RT \left(1 + \frac{d \ln f}{d \ln C} \right) \nabla \ln C = \nu RT \chi \nabla \ln C \end{aligned} \tag{S9}$$

with $\nu = \nu_p + \nu_n$ and $\chi = 1 + \left(d \ln f / d \ln C \right)$. Note that f is salt activity coefficient and C is salt concentration. f is in fact made up of individual ionic activity coefficients, f_p, f_n. χ is otherwise known as the thermodynamic factor[1, 2].

As mentioned earlier, there are more than one solute species. For such a multicomponent system, transport is dictated by Onsager – Stefan – Maxwell (OSM) relation (essentially a constitutive relation connecting fluxes with concentration gradients):

$$-\frac{C_i C_T}{RT} \nabla \mu_i = \sum_{j, j \neq i} \left(\frac{C_j N_i - C_i N_j}{\mathcal{D}_{ij}} \right) \tag{S10}$$

The binary diffusivity tensor $\mathcal{D}_{ij}$ is symmetric, i.e., only three independent diffusivities, namely $\mathcal{D}_{ps}$: cationic diffusivity in the solvent, $\mathcal{D}_{ns}$: anionic diffusivity in the solvent and $\mathcal{D}_{pn}$: mutual diffusivity of cationic – ionic species. Thus, for the electrolyte system under consideration, one has to explicitly measure four properties: $\chi, \mathcal{D}_{ps}, \mathcal{D}_{ns}, \mathcal{D}_{pn}$. However, it is quite difficult to individually study ionic motion as the electrolyte solution is charge neutral for most practical length scales (except recent NMR measurements[3, 4]). The concentrated solution theory is a formalism which appropriately converts these immeasurable properties into measurable transport properties: salt diffusivity - D, transference number - t_p, ionic conductivity - κ and diffusional conductivity - κ_D. As this alternate set is measured, the respective transport relations are used in the mathematical description.

Even if one can write three OSM relations for each of the three species (*p*, *n* or *s*), only two of these are independent as the Gibbs – Duhem does not let all potentials be set independently. Given the interest in the ionic species, the solvent is treated as the reference phase to identify species flux. This is often stated as "carrying out calculations in the solvent frame"[1]. Solvent flux, $N_s = C_s u_s$ where u_s is solvent velocity. This is the bulk velocity and will contribute in the presence of solvent flow, e.g., redox flow battery[5].

$$-\frac{C_p C_T}{RT}\nabla\mu_p = \frac{C_n N_p - C_p N_n}{\mathcal{D}_{pn}} + \frac{C_s N_p - C_p C_s u_s}{\mathcal{D}_{ps}} \tag{S11}$$

$$-\frac{C_n C_T}{RT}\nabla\mu_n = \frac{C_p N_n - C_n N_p}{\mathcal{D}_{pn}} + \frac{C_s N_n - C_n C_s u_s}{\mathcal{D}_{ns}} \tag{S12}$$

With rearrangement:

$$N_p\left(\frac{C_n}{\mathcal{D}_{pn}} + \frac{C_s}{\mathcal{D}_{ps}}\right) - N_n\left(\frac{C_p}{\mathcal{D}_{pn}}\right) = -\frac{C_p C_T}{RT}\nabla\mu_p + \frac{C_p C_s}{\mathcal{D}_{ps}}u_s \tag{S13}$$

$$-N_p\left(\frac{C_n}{\mathcal{D}_{pn}}\right) - N_n\left(\frac{C_p}{\mathcal{D}_{pn}} + \frac{C_s}{\mathcal{D}_{ns}}\right) = -\frac{C_n C_T}{RT}\nabla\mu_n + \frac{C_n C_s}{\mathcal{D}_{ns}}u_s \tag{S14}$$

Note that $C_T = C_p + C_n + C_s$ is total concentration. Further, a solvent contribution can be eliminated from the above two expressions as $\frac{C_n}{\mathcal{D}_{ns}}\times(\text{S13}) - \frac{C_p}{\mathcal{D}_{ps}}\times(\text{S14})$:

$$N_p\left(\frac{C_n C_p}{\mathcal{D}_{ps}\mathcal{D}_{pn}} + \frac{C_n C_n}{\mathcal{D}_{ns}\mathcal{D}_{pn}} + \frac{C_n C_s}{\mathcal{D}_{ps}\mathcal{D}_{ns}}\right) - N_n\left(\frac{C_p C_p}{\mathcal{D}_{ps}\mathcal{D}_{pn}} + \frac{C_p C_n}{\mathcal{D}_{ns}\mathcal{D}_{pn}} + \frac{C_p C_s}{\mathcal{D}_{ps}\mathcal{D}_{ns}}\right)$$
$$= -\frac{\nu_n C_p C_T}{RT}\left(\frac{1}{\mathcal{D}_{ns}}\nabla\mu_p - \frac{1}{\mathcal{D}_{ps}}\nabla\mu_n\right)$$

$$\therefore N_n = \frac{\nu_n}{\nu_p}N_p + \frac{C_T}{RT}\cdot\frac{\left\{\left(\frac{C_p}{\mathcal{D}_{ps}} + \frac{C_n}{\mathcal{D}_{ns}}\right)\nabla\mu_p - \frac{C}{\mathcal{D}_{ps}}\nabla\mu\right\}}{\left(\frac{C_p}{\mathcal{D}_{ps}\mathcal{D}_{pn}} + \frac{C_n}{\mathcal{D}_{ns}\mathcal{D}_{pn}} + \frac{C_s}{\mathcal{D}_{ps}\mathcal{D}_{ns}}\right)} \tag{S15}$$

where $\nabla\mu = \nu_p\nabla\mu_p + \nu_n\nabla\mu_n$ is used to eliminate gradient in anion electrochemical potential, μ_n. Substituting (S15) in (S13):

$$N_p = -\frac{C_p C_T}{RT\mathcal{D}_{pn}(\ )}\nabla\mu - \frac{C_p C_T}{RT\mathcal{D}_{ns}(\ )}\nabla\mu_p + C_p u_s \tag{S16}$$

where $(\ ) \equiv \left(\frac{C_p}{\mathcal{D}_{ps}\mathcal{D}_{pn}} + \frac{C_n}{\mathcal{D}_{ns}\mathcal{D}_{pn}} + \frac{C_s}{\mathcal{D}_{ps}\mathcal{D}_{ns}}\right)$.

Ionic current is given by:

$$I = z_p F N_p + z_n F N_n \tag{S17}$$

Substituting for N_p and N_n (equations S15 and S16):

$$I = -\kappa \nabla \phi - \kappa_D \nabla \ln C \tag{S18}$$

$$\kappa = -z_n F^2 \cdot \frac{CC_T}{RT}\left(\frac{\nu_p}{\mathcal{D}_{ps}} + \frac{\nu_n}{\mathcal{D}_{ns}}\right) / (\ ) \tag{S19}$$

$$\kappa_D = z_n \cdot \frac{CC_T}{RT} \cdot \frac{F}{\mathcal{D}_{ps}} \cdot \nu RT \chi / (\ ) \tag{S20}$$

Replacing $\nabla \mu_p = F \nabla \phi$ in (S16) with (S18):

$$N_p = -\nu_p D \nabla C + t_p \frac{I}{z_p F} + \nu_p C u_s \tag{S21}$$

$$D = \frac{\nu C_T \chi}{(\ )}\left\{\frac{1}{\mathcal{D}_{pn}} + \frac{1}{\nu_p \mathcal{D}_{ns} + \nu_n \mathcal{D}_{ps}}\right\} \tag{S22}$$

$$t_p = \frac{\nu_n / \mathcal{D}_{ns}}{\left(\nu_p / \mathcal{D}_{ps}\right) + \left(\nu_n / \mathcal{D}_{ns}\right)} \tag{S23}$$

Equivalently, the anionic flux can be obtained by substituting N_p (S21) in I (S17):

$$N_n = \frac{I}{z_n F} - \frac{z_p}{z_n} N_p \tag{S24}$$

$$\therefore N_n = \frac{I}{z_n F} - \frac{z_p}{z_n}\left(-\nu_p D \nabla C + t_p \frac{I}{z_p F} + \nu_p C u_s\right) = -\nu_n D \nabla C + \left(1 - t_p\right)\frac{I}{z_n F} + \nu_n C u_s \tag{S25}$$

In summary, one requires the knowledge of four independent properties - D, t_p, κ and κ_D to thoroughly characterize a typical Li-ion battery electrolyte (e.g. [6]). Given the local charge neutrality, one often uses one of the fluxes and ionic current expression for the transport description. In LIBs, since Li^+ is the ion of choice, equations (S18) and (S21) are used as representative transport laws. Note that the salt diffusivity, D, has contributions from all the binary diffusivities as well as the thermodynamic factor. The elegance of this theory lies in the fact that one need not back-compute 'elemental' properties (i.e., $\mathcal{D}_{ps}, \mathcal{D}_{ns}, \mathcal{D}_{pn}, \chi$) and a measurement of composite properties D, t_p, κ, κ_D is sufficient. This is also mathematically efficient as one need not explicitly worry about anion transport.

As a side note, a dilute solution theory employs Nernst – Planck relations to express ionic fluxes (i.e., the constitutive relation). Such a description does neither account for interspecies interaction (resulting from cross-diffusion, e.g., $\mathcal{D}_{pn}$) nor intraspecies interaction (resulting from activity coefficient/ thermodynamic factor).

S2. Electrochemical Response of a Double Layer

The assumption of local charge neutrality is in general not valid near a solid – electrolyte interface. Ionic species often get preferentially adsorbed at the interface and to counter this charged surface, the electrolyte in the close proximity adopts an opposite charge (often referred to as the screening charge). Such an ordering spans a couple of nanometers and the relevant length scale is commonly referred to as the Debye length[1, 7]. This confined structure incorporates the Helmholtz planes and the diffuse layer (which contains the screening charge) and is referred to as the (electrochemical) double layer. Notice that the charge separation takes place within this space and as a whole (i.e., globally) the double layer is charge neutral (equivalent to saying that the capacitor is charge neutral with identical but opposite charges on either plates[8]). This is different than both the bulk phases (solid and electrolyte) which are both globally as well as locally charge neutral.

In porous electrodes, the electrode-electrolyte interface is present throughout the electrode volume. Hence, the double layer dynamics is to be appropriately scaled up to the representative elementary volume length scale. Following up the same notation as earlier, the adsorbed charge is:

$$q^{ad} = z_p F c_p^{ad} + z_n F c_n^{ad} = -q^{sc} \tag{S26}$$

where the first equality follows from the Faraday's law[1], while the second one expresses the global charge neutrality of the double layer, i.e., $q^{ad} + q^{sc} = 0$. Note that the lower-case concentration c's are area specific, i.e., in mol/m^2, in contrast to the volumetric counterparts used in transport discussion (C's are expressed in mol/m^3). Effectively, $c = \int C \, \mathrm{d}x$ with integration being carried out over the adsorbed or screen layers. The screening charge, q^{sc}, is correlated to corresponding ionic concentrations as:

$$q^{sc} = z_p F c_p^{sc} + z_n F c_n^{sc} \tag{S27}$$

Total salt concentration in the double layer is:

$$c = \frac{c_p^{ad} + c_p^{sc}}{\nu_p} = \frac{c_n^{ad} + c_n^{sc}}{\nu_n} \tag{S28}$$

The statement of global double layer charge neutrality, in fact, follows from (S3) and (S28):

$$q^{ad} + q^{sc} = z_p F \left(c_p^{ad} + c_p^{sc} \right) + z_n F \left(c_n^{ad} + c_n^{sc} \right) = \left(\nu_p z_p + \nu_n z_n \right) F c = 0 \tag{S29}$$

In general, both the ionic species can be present in 'adsorbed' as well as 'screening' states. Hence, total salt concentration in a double layer, c, and double layer charge, q^{ad} (or equivalently q^{sc}) are not one-to-one related. Let $\tilde{c}$ be the charge corresponding to the degree of non-neutrality as:

$$\tilde{c} = \frac{c_p^{ad}}{\nu_p} - \frac{c_n^{ad}}{\nu_n} \tag{S30}$$

If cations adsorb more than the anions, $\tilde{c}$, is positive, else it is negative. $\tilde{c}=0$ signifies identical adsorption for both the ions. Substituting for c_p^{ad} in (S26):

$$q^{ad} = z_p F c_p^{ad} + z_n F c_n^{ad} = z_p F\left(\nu_p \tilde{c} + \frac{\nu_p c_n^{ad}}{\nu_n}\right) + z_n F c_n^{ad} = \nu_p z_p F \tilde{c} \tag{S31}$$

Equivalently, it can be shown that,

$$q^{sc} = \nu_n z_n F \tilde{c} \tag{S32}$$

Thus, concentration $\tilde{c}$ directly correlates to the amount of charge separated (equivalently stored) in the double layer. Consequently, the total salt concentration in the double layer is:

$$c = \frac{c_p^{ad} + c_p^{sc}}{\nu_p} = \left(\frac{c_p^{ad}}{\nu_p} - \frac{c_n^{ad}}{\nu_n}\right) + \frac{c_p^{sc}}{\nu_p} + \frac{c_n^{ad}}{\nu_n} = \tilde{c} + \frac{c_p^{sc}}{\nu_p} + \frac{c_n^{ad}}{\nu_n}$$

Let neutral salt concentration in the 'adsorbed' and 'screened' states be c^{ad} and c^{sc}, respectively. Hence, the above expression can be simplified as:

$$c = \tilde{c} + c^{ad} + c^{sc} \tag{S33}$$

Equation (S33) divides the total salt concentration in the double layer into three forms: $\tilde{c}$ related to stored charge, and c^{ad}, c^{sc} which characterize the portions of adsorbed (and screened) ions that nullify each other. Based on charge measurements, $\tilde{c}$ can be back inferred, while the other two cannot be so easily detected. Here on it is often assumed that cation is present in the adsorbed state, while anion is the screening charge[9]. This makes $c^{ad} = c^{sc} = 0$, and double layer charge and salt concentration become uniquely related:

$$q^{ad} = \nu_p z_p F c \tag{S34}$$

This assumption is important since the electrolyte species balance is expressed in terms of salt concentration. The adsorbed charge relates to the potential drop between the (bulk) electrode and (bulk) electrolyte as, with $\mathcal{C}_{dl}$ being area specific double layer capacitance – measured in F/m^2:

$$q = \mathcal{C}_{dl}\left(\phi_s - \phi_e\right) \tag{S35}$$

Or, in terms of charging/ discharging:

$$\frac{dq}{dt} = \mathcal{C}_{dl}\frac{d\left(\phi_s - \phi_e\right)}{dt} \tag{S36}$$

Here it is assumed that the double layer capacitance, $\mathcal{C}_{dl}$ is not a function of salt concentration or potentials. Combining, (S34) and (S36):

$$\frac{dq}{dt} = \mathcal{C}_{dl}\frac{d\left(\phi_s - \phi_e\right)}{dt} = \nu_p z_p F \frac{dc}{dt} \tag{S37}$$

dc/dt can be interpreted as salt flux into the double layer, per unit electrode – electrolyte surface. For a porous electrode, the equivalent volumetric form is:

$$\frac{dQ}{dt} = a_0 \mathcal{C}_{dl} \frac{d\left(\phi_s - \phi_e\right)}{dt} = \nu_p z_p F a_0 \frac{dc}{dt} = \nu_p z_p F \frac{dC}{dt} \tag{S38}$$

where Q is charge stored in double layer per unit electrode volume, a_0 is electrode – electrolyte interfacial area and C is a salt concentration in the double layer per unit electrode volume. A positive dQ/dt signifies charging of the electrochemical double layer and is equivalent to the charging current. When current dQ/dt is passed, cations (in the present context) get adsorbed at a rate $dC_p / dt = \nu_p dC / dt$, and correspondingly anions arrange in the diffuse layer to screen this charge.

Sign convention:

There are two forms of current at the electrochemically active interface – faradic (related to electrochemical reactions; here intercalation) and capacitive (related to double layer charging). The faradic current is considered positive when cations are generated in the electrolyte (i.e., the deintercalation process). Double layer charging in a given electrode volume implies, accumulation of additional ions at the active interface. To be consistent with the sign convention of the faradic current, capacitive current is considered positive when it stores more ions. Mathematically,

$$j_c = \frac{dQ}{dt} = a_0 \mathcal{C}_{dl} \frac{d\left(\phi_s - \phi_e\right)}{dt} \tag{S39}$$

with Q being the double layer charge. Thus, the salt concentration can increase due to ionic flux (diffusive, migrative or advective), electrochemical reactions and double layer charging. The net salt concentration, C, in a given electrode volume implicitly accounts for the charge stored in the double layer as well and one does not require independent species balance equation.

$$\therefore \varepsilon \frac{\partial C_p}{\partial t} = -\nabla \cdot N_p + \left(r_f + r_c\right) \tag{S40}$$

where r_f is generation term from the faradic current and r_c for the double layer charging. Equivalent charge balance is:

$$-\nabla \cdot I + \left(j_f + j_c\right) = 0 \tag{S41}$$

Since, intercalation reaction is always expressed as the generation of one Li^+, $r_f = j_f/z_pF$. And, $r_c = j_c/z_pF$. With these substitutions, (S40) simplifies to,

$$\varepsilon \frac{\nu_p \partial C}{\partial t} = \nu_p \nabla \cdot \left(D \frac{\varepsilon}{\tau} \nabla C \right) - \frac{1}{z_p F} \nabla \cdot \left(t_p I\right) + \frac{j_f}{z_p F} + \frac{j_c}{z_p F} \tag{S42}$$

$$\therefore \varepsilon \frac{\nu_p \partial C}{\partial t} = \nu_p \nabla \cdot \left(D \frac{\varepsilon}{\tau} \nabla C \right) - \frac{t_p}{z_p F} \left(j_f + j_c \right) + \frac{j_f}{z_p F} + \frac{j_c}{z_p F} \tag{S43}$$

$$\therefore \varepsilon \frac{\nu_p \partial C}{\partial t} = \nu_p \nabla \cdot \left(D \frac{\varepsilon}{\tau} \nabla C \right) + \frac{j_f}{z_p F} \left(1 - t_p\right) + \frac{j_c}{z_p F} \left(1 - t_p\right) \tag{S44}$$

where transference number, t_p, is fairly constant over a wide range of concentrations and its spatial dependence can be neglected (going from (S42) to (S43)). For Li^+, $z_p = 1$, and for a typical salt such as $LiPF_6$, $\nu_p = 1$. This simplifies (S44) as:

$$\varepsilon \frac{\partial C}{\partial t} = \nabla \cdot \left(D \frac{\varepsilon}{\tau} \nabla C \right) + \frac{\left(1 - t_p\right)}{F} j \tag{S45}$$

and charge balance in solid and electrolyte phases as:

$$\nabla \cdot \left(\kappa \frac{\varepsilon}{\tau} \nabla \phi_e \right) + \nabla \cdot \left(\kappa_D \frac{\varepsilon}{\tau} \nabla \ln C \right) + j = 0 \tag{S46}$$

$$\sigma^{\text{eff}} \nabla^2 \phi_s = j \tag{S47}$$

where intercalation and double layer charging terms are grouped together as $j = j_f + j_c$. Note that for transport through porous electrodes, porosity and tortuosity terms appear as pre-factors. In most of the existing literature (except[9, 10]), the origins of the double layer impedance are not explained. The preceding discussion is incorporated so as to revisit the specific details of double layer description, specifically the associated assumptions.

S3. Mathematical Details of Electrode Impedance

For the most part, literature analyzes the impedance data via circuit-based models[11-18], except a few works[9, 19-21]. At best this sort of interpretation identifies the order of various transport processes but offers little insights into microstructural details or spatial coupling of different resistive modes. For a typical electrode, lateral dimensions are quite larger than the thickness, hence the derivative operator, ∇, needs to be expressed in this direction. Accounting for the intercalation based *Li* storage in active material particles, the electrochemical response of a porous intercalation electrode is mathematically described by the following set of governing equations. Subscripts '*s*' and '*e*' denote solid and electrolyte phase properties, respectively.

Li storage in active material particles:

$$\frac{\partial C_s}{\partial t} = \frac{1}{r^2} \frac{\partial}{\partial r} \left(D_s r^2 \frac{\partial C_s}{\partial r} \right) \tag{S48}$$

Li^+ transport in the electrolyte phase:

$$\varepsilon \frac{\partial C_e}{\partial t} = \frac{\partial}{\partial x} \left(D_e \frac{\varepsilon}{\tau} \frac{\partial C_e}{\partial x} \right) + \left(\frac{1 - t_p}{F} \right) j \tag{S49}$$

(Electronic) Charge conservation in the solid phase:

$$\sigma^{\text{eff}} \frac{\partial^2 \phi_s}{\partial x^2} = j \tag{S50}$$

(Ionic) Charge conservation in the electrolyte phase:

$$\frac{\partial}{\partial x} \left(\kappa \frac{\varepsilon}{\tau} \frac{\partial \phi_e}{\partial x} \right) + \frac{\partial}{\partial x} \left(\kappa_D \frac{\varepsilon}{\tau} \frac{\partial \ln C_e}{\partial x} \right) + j = 0 \tag{S51}$$

As discussed earlier, the electrolyte transport description is in accordance with the concentrated solution theory[1, 2]. Transport of both anion and cation take place in such liquid electrolytes, and

given the local charge neutrality, only cation transport (S49) is explicitly followed in the present discussion. Porosity (ε), tortuosity (τ) and effective electronic conductivity (σ^{eff}) appearing in these expressions account for electrode microstructural effects. Additionally, electrochemically active area factors in this electrochemical response when charge conversion from electronic to ionic or vice versa (i.e., electrochemical reaction flux) is considered. Volumetric current source term, j , quantifies the reactions taking place at the RVE scale, and has both faradic and capacitive contributions, i.e., $j = j_f + j_c$. The faradic (or intercalation) term has the following functional dependence:

$$j_f = ak\sqrt{C_s^f C_e \left(C_s^{max} - C_s^f\right)}\left\{e^{\frac{F}{2RT}(\phi_s - \phi_e - U)} - e^{-\frac{F}{2RT}(\phi_s - \phi_e - U)}\right\} \tag{S52}$$

As the active material – electrolyte interface is partly covered due to the presence of the CBD phase, this volumetric flux (only the faradic component) has to be appropriately redistributed over the particle surface to ensure flux continuity. Subsequently, the intercalation flux at the active material surface becomes:

$$-D_s \frac{\partial C_s}{\partial r}\bigg|_{r=R_p} = \frac{j_f}{a_0 F} \tag{S53}$$

where $a_0 = 3\varepsilon_s / R_p$ is the theoretical active area. The capacitive flux results from double layer charging/ discharging at the solid – electrolyte interface. Double layer as a whole is charge neutral[1] and accordingly, its participation can be quantified as a flux of either of the ions. Here electrolyte interactions are presented in the form of cation transport (S49) and ionic charge balance (S51).

The microstructural properties have been characterized based on pore-scale analysis of composite electrode. Based on these calculations, relevant properties such as tortuosity, conductivity, and electrochemically active area have been expressed as functions of electrode recipe. Interested readers are encouraged to read[22, 23]. These expressions detail the electrode response in the time domain. These governing equations are transformed to the frequency domain using the Laplace transform. The mathematical treatment is similar to that carried out earlier[21, 24, 25] with advances made to account for electrode microstructural properties coming from pore-scale calculations. First, the equations are linearized around an equilibrium state (impedance measurements are often carried out in the rest phase). This leads to the following forms of equations (S48) to (S52):

$$\frac{\partial c'_s}{\partial t} = \frac{D_s}{r^2}\frac{\partial}{\partial r}\left(r^2 \frac{\partial c'_s}{\partial r}\right) \tag{S54}$$

$$\varepsilon \frac{\partial c'_e}{\partial t} = D_e \frac{\varepsilon}{\tau}\frac{\partial^2 c'_e}{\partial x^2} + \left(\frac{1 - t_p}{F}\right) j' \tag{S55}$$

$$\sigma^{\text{eff}} \frac{\partial^2 \phi'_s}{\partial x^2} = j' \tag{S56}$$

$$\kappa \frac{\varepsilon}{\tau}\frac{\partial^2 \phi'_e}{\partial x^2} + \frac{\kappa_D}{C_e}\cdot\frac{\varepsilon}{\tau}\frac{\partial^2 c'_e}{\partial x^2} + j' = 0 \tag{S57}$$

$$j'_f = a\left[k\sqrt{C_s^f C_e\left(C_s^{max} - C_s^f\right)}\right]\frac{F}{RT}\left(\phi'_s - \phi'_e - c'^f_s \frac{\partial U}{\partial C_s}\right) \tag{S58}$$

where transport properties and rate constants are computed using equilibrium state concentrations and potentials (refer to Table S1 for values). All the dashed quantities correspond to fluctuations around the respective rest phase properties. Note that expression (S58) is the faradic current, i.e., associated with electrochemical reactions. The terms inside the square brackets refer to exchange current density, that is dependent on the lithiation extent.

$$i_0\left(C_s\right) = k\sqrt{C_s C_e\left(C_s^{max} - C_s\right)} \tag{S59}$$

An additional current contribution arises from charging/ discharging of the double layer capacitor associated with the electrified interface[1, 7, 9], and is expressed as follows (assuming that the capacitance is same for the active material – electrolyte and CBD – electrolyte interfaces):

$$j'_c = a_0 \boldsymbol{e}_{dl} \frac{d\left(\phi'_s - \phi'_e\right)}{dt} \tag{S60}$$

Net volumetric current appearing at the RVE scale is $j' = j'_f + j'_c$. Taking the Laplace transform of expression (S54) and using the rule for the transform of differentiation[26], the following ordinary differential equation results ($s = i\omega$):

$$\frac{1}{r^2}\frac{d}{dr}\left(r^2 \frac{d\tilde{c}_s}{dr}\right) - \left(\frac{s}{D_s}\right)\tilde{c}_s = 0$$

whose solution is (where $\lambda^2 = s / D_s$):

$$\tilde{c}_s = \frac{A}{r}\sinh\left(\lambda r\right)$$

Note that boundary condition at the particle center (that the concentration should be finite) has been used. The remaining integration constant – A, shall be identified using the interface condition (frequency domain counterpart of expression S53):

$$A = \frac{\frac{a i_0}{a_0 RT}\left(\tilde{\phi}_s - \tilde{\phi}_e\right)}{\left\{\frac{1}{R_p}\sinh\left(\lambda R_p\right)\left(\frac{a i_0}{a_0 RT}\cdot\frac{\partial U}{\partial C_s} + \frac{D_s}{R_p}\right) - \frac{\lambda D_s}{R_p}\cosh\left(\lambda R_p\right)\right\}} \tag{S61}$$

Subsequently, the volumetric faradic current (Eq. S58) is:

$$\tilde{j}_f = \frac{\tilde{\phi}_s - \tilde{\phi}_e}{\left\{\frac{a_0}{a}R_{ct} + \frac{1}{a_0}\cdot\frac{\partial U}{\partial C_s}\cdot\frac{R_p}{F D_s}\cdot\frac{\tanh\left(\lambda R_p\right)}{\tanh\left(\lambda R_p\right) - \left(\lambda R_p\right)}\right\}} = \frac{\tilde{\phi}_s - \tilde{\phi}_e}{Z_f} \tag{S62}$$

with $R_{ct} = RT / a_0 i_0 F$. Both the capacitive and faradic currents flow in parallel, resulting in the following form of the interfacial impedance at the RVE scale:

$$\tilde{j} = \tilde{j}_f + \tilde{j}_c = \frac{\tilde{\phi}_s - \tilde{\phi}_e}{Z_f} + \frac{\tilde{\phi}_s - \tilde{\phi}_e}{Z_c} = \frac{\tilde{\phi}_s - \tilde{\phi}_e}{Z_i} \tag{S63}$$

where $Z_c = 1/a_0 i\omega \mathcal{C}_{dl}$ and $Z_i = Z_f Z_c / \left(Z_f + Z_c\right)$.

Note that this derivation assumes a monodisperse active material particle system since the motivation for the present study is to understand the coupling of RVE scale effects and their upscaling to the electrode scale. The complexations arising in the intercalation dynamics due to particle size distribution are fairly straightforward[21].

Given the analytical expression (S63) for the interfacial impedance, the set of equations describing the electrode scale impedance reduces to the following:

$$s\varepsilon\tilde{c}_e = D_e \frac{\varepsilon}{\tau}\frac{d^2\tilde{c}_e}{dx^2} + \left(\frac{1-t_p}{F}\right)\tilde{j} \tag{S64}$$

$$\sigma^{\text{eff}}\ \frac{d^2\tilde{\phi}_s}{dx^2} = \tilde{j} \tag{S65}$$

$$\kappa\frac{\varepsilon}{\tau}\frac{d^2\tilde{\phi}_e}{dx^2} + \frac{\kappa_D}{C_e}\cdot\frac{\varepsilon}{\tau}\frac{d^2\tilde{c}_e}{dx^2} + \tilde{j} = 0 \tag{S66}$$

along with the set of boundary conditions:

electrode – separator boundary	*electrode – current collector boundary*	
$-D_e\frac{\varepsilon}{\tau}\frac{d\tilde{c}_e}{dx} = \frac{\left(1-t_p\right)}{F}\tilde{I}_{app}$	$\frac{d\tilde{c}_e}{dx} = 0$	(S67)
$-\kappa\frac{\varepsilon}{\tau}\frac{d\tilde{\phi}_e}{dx} - \frac{\kappa_D}{C_e}\cdot\frac{\varepsilon}{\tau}\frac{d\tilde{c}_e}{dx} = \tilde{I}_{app}$	$\tilde{\phi}_e = 0$	(S68)
$\frac{d\tilde{\phi}_s}{dx} = 0$	$-\sigma^{\text{eff}}\ \frac{d\tilde{\phi}_s}{dx} = \tilde{I}_{app}$	(S69)

The specification of these boundary conditions is critical to quantification of the electrode impedance spectra. Experimentally electrode impedance is measured in a half-cell setting where the test electrode is set against Li metal anode and the two are separated by a porous separator[12]. At the anode-separator interface, applied current translates to ionic current. No electrochemical reactions take place inside the separator and in turn, the ionic fluxes remain invariant across the separator (this does allow a concentration profile to evolve such that the ionic fluxes are spatially invariant). At anode-separator interface, Li^+ ions are generated. This leads to the flux balance: $N = -D_e\frac{\varepsilon}{\tau}\frac{\partial C_e}{\partial x} + \frac{t_p}{F}I_{app} = \frac{I_{app}}{F} \Rightarrow -D_e\frac{\varepsilon}{\tau}\frac{\partial C_e}{\partial x} = \frac{\left(1-t_p\right)}{F}I_{app}$. Also, the ionic current at any location in the separator is equal to the total current being passed through the cell, i.e., $I_{app} = -\kappa\frac{\varepsilon}{\tau}\frac{\partial\phi_e}{\partial x} - \kappa_D\frac{\varepsilon}{\tau}\frac{\partial\ln C_e}{\partial x}$. Since no electronic current can enter through the separator – cathode interface, corresponding gradient in the solid phase potential is set to zero in expression (S68). On the other hand, the current collector is impervious to ionic flux, i.e., $\partial C_e \big/ \partial x = 0$. To make the set of governing equations well-posed, one has to fix one of the potentials. Electrolyte

phase potential is fixed at the current collector boundary (S68). At current collector, all the current becomes electronic in nature and equation (S69) ensures this physics.

The set of ordinary differential equations (S64) to (S66) along with the boundary conditions (S67) to (S69) are numerically solved. Afterward, the electrode impedance is computed as the equation:

$$Z_{electrode} = \frac{\tilde{\phi}_s\left(x=L\right) - \tilde{\phi}_e\left(x=0\right)}{\tilde{I}_{app}} \qquad \text{(S70)}$$

Here $\tilde{I}_{app}$ is applied current density (A/m^2) in the frequency domain. Note that this is the impedance of the porous electrode only. Experimentally one uses a half-cell setup in order to measure the electrode impedance. A half-cell configuration involves a Li metal anode, suitable separator and the test porous electrode. The half-cell impedance involves contributions from the interfacial impedance of Li metal anode as well as ionic transport resistance of separator (a function of separator microstructure), in addition to the electrode impedance. One needs to carry out further post-processing steps on experimentally measured impedance spectrum (i.e., a half-cell) in order to extract electrode only impedance.

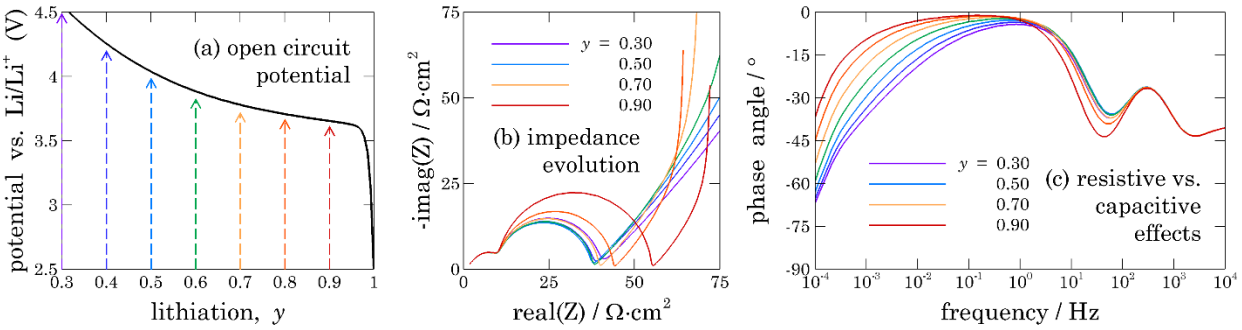

Figure S1*: Lithiation dependence stems from changes in exchange current density and electrode potential with intercalation (a). This directly correlates to interfacial effects and accordingly, the lower frequency behavior (b) and (c) changes with lithiation.*

Figure S1 reports the evolution of impedance with lithiation, for 50 μm thick porous intercalation electrodes with Nickel Cobalt Manganese oxide (NCM 333) active material, acetylene black conductive additives and poly (vinyldenedifluoride) binder in proportional 95 : 2.5 : 2.5 by weight and 25 % porosity. The active material particles have a mean particle radius of 5 μm. Relevant material properties have been borrowed from literature and have also been listed in authors' earlier articles[22, 23]. The respective microstructural properties have been estimated based on the effective property relations reported recently[22]. With lithiation (Figure S1(a)), the interfacial impedance changes in response to changes in the exchange current density as well as the slope of the open circuit potential profile (S61), while the microstructural properties stay unchanged. Corresponding impedance spectra are sketched in Figure S1(b) and report the variation of impedance over a range of excitation frequencies 0.1 mHz to 10 kHz. General nature of the impedance plot (Figure S1 (b)) shows two smoothly joined circular portions and a low-frequency tail. Since the impedance in

intercalation electrodes has contributions from various resistive mechanisms and double layer capacitance, corresponding phase angle quantitatively isolates the relative contribution of these effects (Figure S1 (c)). The closer the phase angle to zero, the greater is the resistive contribution. Figure S1 (c) reveals that changes in lithiation only affects the lower frequency impedances, while the higher frequency response stays invariant. In other words, the higher frequency behavior is dominated by interactions not associated with intercalation. These higher frequencies, in fact, probe the transport characteristics. Interestingly, even at much higher frequencies, the phase angle is not zero, suggesting that the double layer charging does contribute in this range. This joint interplay between double layer effects and transport resistances (both ionic and electronic) give rise to the second high-frequency semi-circle as apparent in Figure S1 (b). Note that this feature appears in the frequency range of 0.1 – 10 kHz.

Table S1*: A summary of physical properties along with their description, values, and functional dependences.*

Property	*Description*	*Units*
a	Electrochemically active area	m^2/m^3
a_0	Theoretical electrochemically active area	m^2/m^3
$\mathcal{C}_{dl}$	Double layer capacitance (0.1)	F/m^2
C_e	Li^+ concentration in electrolyte (1200.0)	mol/m^3
C_s	Li concentration in active material particle (max = 49500.0)	mol/m^3
D_s	Diffusivity for Li intercalation in active material (3.0×10^{-15})	m^2/s
D_e	Diffusivity for Li^+ transport in bulk electrolyte $D_e\left(C_e,T\right)=10^{-\left\{8.43+\frac{54}{\left(T-229-5C_e/1000\right)}-\left(0.22C_e/1000\right)\right\}}$	m^2/s
F	Faraday's constant (96487)	C/mol
i_0	Exchange current density for intercalation reaction (per unit area of the electrochemically active interface)	A/m^2
I_{app}	Applied current density	A/m^2
j	Volumetric current	A/m^3
k	Reaction rate constant (2.3327×10^{-6})	$A/m^2(mol/m^3)^{3/2}$
L	Electrode thickness	m
r	Radial coordinate – along the active material particle radius	m
R_p	Particle radius (5.0×10^{-6})	m
R	Universal gas constant (8.314)	J/mol·K
t	Time	s
t_p	Transference number (0.38)	-
T	Temperature of operation (298)	K
U	Open circuit potential for electrode active material (here NCM) $U\left(y\right)=6.0826-6.9922y+7.1062y^2-2.5947y^3$ $-5.4549\times10^{-5}\exp\left(124.23y-114.2593\right)$	V

x	Spatial coordinate – along electrode thickness $x=0$: separator – electrode interface $x=L$: electrode – current collector interface	m
y	Intercalation fraction in active material: $y=C_s/C_s^{max}$	-
Z	(area specific) impedance	$\Omega\cdot m^2$
Greek symbols:		
ε	Porosity/ electrolyte volume	m^3/m^3
ϕ_e	Electric potential in the electrolyte phase	V
ϕ_s	Electric potential in the solid phase	V
κ	Ionic conductivity of bulk electrolyte	S/m
	$\kappa(C_e,T)=10^{-4}C_e\left\{\begin{array}{l}-10.5+0.668C_e/1000+0.494C_e^2/1000^2\\ +0.074T-0.0178TC_e/1000-8.86\times10^{-4}TC_e^2/1000^2\\ -6.96\times10^{-5}T^2+2.80\times10^{-5}T^2C_e/1000\end{array}\right\}^2$	
κ_D	Diffusional conductivity of bulk electrolyte	A/m
	$\frac{-F\kappa_D}{2RT\kappa}=0.601-0.240\sqrt{C_e/1000}+0.982\left(1-0.0052(T-294)\right)\sqrt{\left(C_e/1000\right)^3}$	
σ^{eff}	Effective electronic conductivity of composite electrode	S/m
τ	Tortuosity of electrolyte-filled pore network	m/m
ω	Excitation frequency	rad/s
Superscripts:		
‘	Departure from equilibrium state	
~	Frequency domain variable for the corresponding time domain variable	
Abbreviations:		
CBD	Conductive Binder Domains	
NCM	Nickel Cobalt Manganese oxide	
RVE	Representative Volume Element	

S4. Impedance for a Multivalent Intercalation Chemistry

If the ionic charge on the cation is higher than 1+, the previous set of equations have to be appropriately revised. Specifically, a higher valence cation exhibits a smaller molar flux, subsequently reducing the diffusional impedance (S62):

$$Z_f=\frac{a_0}{a}R_{ct}+\frac{1}{z_p a_0}\cdot\frac{\partial U}{\partial C_s}\cdot\frac{R_p}{FD_s}\cdot\frac{\tanh\left(\lambda R_p\right)}{\tanh\left(\lambda R_p\right)-\left(\lambda R_p\right)} \tag{S71}$$

This effectively increases the capacitive contribution and the low-frequency diffusional tail demonstrates a greater slope on the impedance profile as apparent in Figure S2. Another

representative change occurs for the electrolyte transport (refer equation (S23)), where a multivalent cation has a higher transference number:

$$t_p = \frac{\nu_n / \mathcal{D}_{ns}}{\left(\nu_p / \mathcal{D}_{ps}\right) + \left(\nu_n / \mathcal{D}_{ns}\right)} = \frac{z_p \mathcal{D}_{ps}}{z_p \mathcal{D}_{ps} - z_n \mathcal{D}_{ns}} \tag{S72}$$

Note that the diffusivities in the above expression also change in response to changes in ionic radii as well as background solvent. This A higher transference number implies that the contribution of cationic flux to total current increases[1, 27], and effectively the electrolyte phase potential drop decreases. This attenuates the second – higher frequency semicircle (Figure S2). Figure S2 sketches these qualitative differences among the intercalation response with multivalent cations.

$$s\varepsilon\tilde{c}_e = D_e \frac{\varepsilon}{\tau} \frac{d^2\tilde{c}_e}{dx^2} + \left(\frac{1 - t_p}{\nu_p z_p F} \right) \tilde{j} \tag{S73}$$

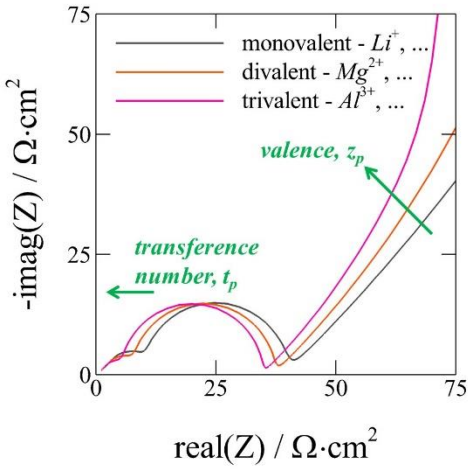

Figure S2*: As cationic charge increases; diffusional impedance decreases which result in a higher slope low-frequency tail. Moreover, a multivalent cation has a greater transference number and in turn, electrolyte transport resistance decreases. Here material nonlinearities, e.g., multiphase intercalation, have not been accounted for.*

In addition to these non-monotonic trends, often intercalation for multivalent cations takes place in multiple stages. Such multistage intercalation[28, 29] brings in material nonlinearities and further alters the impedance response.

REFERENCES

1. J. Newman and K. E. Thomas-Alyea, *Electrochemical systems*, John Wiley & Sons, New Jersey, 2012.
2. A. M. Bizeray, D. A. Howey and C. W. Monroe, *J. Electrochem. Soc.*, 2016, **163**, E223-E229.
3. S. U. Kim and V. Srinivasan, *J. Electrochem. Soc.*, 2016, **163**, A2977-A2980.
4. Z. Feng, K. Higa, K. S. Han and V. Srinivasan, *J. Electrochem. Soc.*, 2017, **164**, A2434-A2440.
5. A. Z. Weber, M. M. Mench, J. P. Meyers, P. N. Ross, J. T. Gostick and Q. Liu, *J. Appl. Electrochem.*, 2011, **41**, 1137.
6. L. O. Valøen and J. N. Reimers, *J. Electrochem. Soc.*, 2005, **152**, A882-A891.
7. J. N. Israelachvili, *Intermolecular and surface forces*, Academic press, New York, 2011.
8. J. Walker, *Halliday & Resnick Fundamentals of Physics*, John Wiley & Sons, Incorporated, 2014.
9. M. Doyle, J. P. Meyers and J. Newman, *J. Electrochem. Soc.*, 2000, **147**, 99-110.

10. J. Lück and A. Latz, *Phys. Chem. Chem. Phys.*, 2016, **18**, 17799-17804.
11. H. Zheng, J. Li, X. Song, G. Liu and V. S. Battaglia, *Electrochim. Acta*, 2012, **71**, 258-265.
12. D. Juarez-Robles, C.-F. Chen, Y. Barsukov and P. P. Mukherjee, *J. Electrochem. Soc.*, 2017, **164**, A837-A847.
13. J. Landesfeind, J. Hattendorff, A. Ehrl, W. A. Wall and H. A. Gasteiger, *J. Electrochem. Soc.*, 2016, **163**, A1373-A1387.
14. S. Malifarge, B. Delobel and C. Delacourt, *J. Electrochem. Soc.*, 2017, **164**, E3329-E3334.
15. F. P. McGrogan, S. R. Bishop, Y.-M. Chiang and K. J. Van Vliet, *J. Electrochem. Soc.*, 2017, **164**, A3709-A3717.
16. M. Takeno, T. Fukutsuka, K. Miyazaki and T. Abe, *J. Electrochem. Soc.*, 2017, **164**, A3862-A3867.
17. B. Delattre, R. Amin, J. Sander, J. De Coninck, A. P. Tomsia and Y.-M. Chiang, *J. Electrochem. Soc.*, 2018, **165**, A388-A395.
18. J. Landesfeind, M. Ebner, A. Eldiven, V. Wood and H. A. Gasteiger, *J. Electrochem. Soc.*, 2018, **165**, A469-A476.
19. M. D. Murbach and D. T. Schwartz, *J. Electrochem. Soc.*, 2018, **165**, A297-A304.
20. J. Huang, Z. Li, J. Zhang, S. Song, Z. Lou and N. Wu, *J. Electrochem. Soc.*, 2015, **162**, A585-A595.
21. J. P. Meyers, M. Doyle, R. M. Darling and J. Newman, *J. Electrochem. Soc.*, 2000, **147**, 2930-2940.
22. A. N. Mistry, K. Smith and P. P. Mukherjee, *ACS Appl. Mater. Interfaces*, 2018, **10**, 6317-6326.
23. A. Mistry, D. Juarez-Robles, I. V. M. Stein, K. Smith and P. P. Mukherjee, *J. Electrochem. Energy Convers. Storage*, 2016, **13**, 031006-031006.
24. M. D. Murbach and D. T. Schwartz, *J. Electrochem. Soc.*, 2017, **164**, E3311-E3320.
25. J. Huang and J. Zhang, *J. Electrochem. Soc.*, 2016, **163**, A1983-A2000.
26. E. Kreyszig, *Advanced Engineering Mathematics*, John Wiley & Sons, Singapore, 2010.
27. K. M. Diederichsen, E. J. McShane and B. D. McCloskey, *ACS Energy Lett.*, 2017, **2**, 2563-2575.
28. L. R. De Jesus, J. L. Andrews, A. Parija and S. Banerjee, *ACS Energy Lett.*, 2018, **3**, 915-931.
29. J. L. Andrews, A. Mukherjee, H. D. Yoo, A. Parija, P. M. Marley, S. Fakra, D. Prendergast, J. Cabana, R. F. Klie and S. Banerjee, *Chem*, 2018, **4**, 564-585.